PARAMETER STUDIES ON EMISSIONS AND COSTS OF A PARTIAL TURBOELECTRIC COMMUTER AIRCRAFT

C. Zumegen*, P. Strathoff*, E. Stumpf*
* Institute of Aerospace Systems (ILR), RWTH Aachen University, Aachen

Abstract

The emissions of CO_2 and NO_X and costs are the most important evaluation parameters of novel aircraft propulsion systems. They are consequently considered in a holistic analysis of the electrification of 9- to 50-seater aircraft in the project GNOSIS. Within the project, a partial turboelectric commuter aircraft with 19 seats and electrically driven wingtip propellers was designed in the conceptual aircraft design tool MICADO. The effect of important design parameters (wing aspect ratio, cruise speed and altitude and propeller diameter) on the emissions and costs are presented in this paper. To estimate the life cycle costs of the partial turboelectric aircraft, new cost relationships are derived from existing data in the literature. Even though the wingtip propellers increase the maximum lift to drag ratio of the partial turboelectric aircraft in cruise, the emissions of the unchanged configuration increase by 0.46 % relative to the reference aircraft in a year 2025 scenario. Because different wing aspect ratios, cruise speeds and cruise altitudes lead to the similar effects on the emissions of the conventionally driven and the partial turboelectric aircraft, the electrified aircraft shows no advantages in terms of emission reduction over the conventional aircraft. The additional powertrain components in the partial turboelectric aircraft lead to a moderate change of the total operating costs (-0.29 % to +1.57 %), the recurring costs (+2.07 % to +3.46 %) and non-recurring costs (+1.24 % to +2.51 %).

Keywords

commuter aircraft, electrification, CO_2 and NO_X emissions, life cycle costs

NOMENCLATURE

Symbols

C_P	Power coefficient of the propeller	[-]
C_{Range}	Design range of the aircraft	[NM]
$\frac{C_T}{C_P}$	Ratio of the propeller's thrust and power coefficient	[-]
D	Diameter of the propeller	[m]
$EOLF$	End of life costs	[USD]
FC	Number of flight cycles	[-]
FH	Flight hours	[h]
IOC	Indirect operating costs	[USD]
K	Maintenance cost factor	[-]
LF	Seat load factor	[-]
MC	Maintenance costs	[USD]
m	Mass of the powertrain component	[kg]
$MTOM$	Maximum take off mass	[kg]
n	Rotational speed of the propeller	[1/s]
$N_{Gasturbines}$	Number of gas turbines	[-]
N_{Seat}	Number of seats	[-]
OEM	Operating empty mass	[kg]
P	Shaft power	[W]
p	Price of the powertrain component	[USD]
$\Phi_{Airframe}$	Share of the airframe maintenance that is performed at the operator	[-]
$\Phi_{Gasturbines}$	Share of the gas turbine maintenance that is performed externally	[-]
R	Design range	[NM]
$SLST$	Sea level static thrust	[N]
$W_{Mechanic}$	Hourly wage of a mechanic	[USD]

Abbreviations

CFD	Computational fluid dynamics
CS	Certification Specification
DAPCA	Development and Procurement Cost of Aircraft model of the RAND Corporation
EIS	Entry into service
FAA	U.S. Federal Aviation Administration
LIFTING_LINE	Multi-liftingline tool from the German Aerospace Center
MICADO	Multidisciplinary integrated conceptual aircraft design and optimization tool
PT 2025	Partial turboelectric aircraft in 2025
REF 2025	Reference aircraft in 2025
SFC	Specific fuel consumption [g/kNs]
USD	U.S. dollar
XML	Extensible style sheet language

doi: 10.25967/570139

1. MOTIVATION

Before 2020, CO_2 emissions in the aviation sector increased by 4 % to 5 % per year [1]. Beside the emission of CO_2, also contrail and aviation-induced cloudiness contribute to global warming [2]. The combustion of hydrocarbons or hydrogen within the powertrain of an aircraft leads to emissions during operation, that can include CO_2, NO_X and water. In contrast to that, the electrification of aircraft propulsion can optimally lead to zero emissions during the mission.
Hence, the LuFo-project GNOSIS aims at a holistic analysis of electrified aircraft concepts ranging from 9 to 50 seats. In a first phase of the project, the electrification of a 19-seater commuter aircraft is investigated. The investigation comprises two different time horizons, 2025 and 2050, of which only the first one is considered in this paper. The initial technology selection process for an aircraft design in 2025 resulted in a partial turboelectric commuter aircraft with electrically driven wingtip propellers [3]. After modeling the different technologies in the conceptual aircraft design environment MICADO [3, 4], this paper analyzes the effect of selected design parameters of a partial turboelectric commuter aircraft on the emission of CO_2 and NO_X. Since the aircraft design has to be attractive for potential aircraft operators, new cost relationships for an electrified aircraft will additionally consider the life cycle costs of the electrified aircraft.

2. DESIGN OF THE COMMUTER AIRCRAFT

Publicly available data (pilot operating handbook, three-dimensional drawings) provide the required data to design the 19-seater commuter aircraft in the in-house conceptual aircraft design tool MICADO [5]. At first, a redesign of an existing 19-seater commuter adjusted to technology levels expected in 2025 is done before its electrified version is designed.

2.1. Conceptual aircraft design tool

Over the last years, the Institute of Aerospace Systems has developed an in-house conceptual aircraft design tool, called MICADO (Multidisciplinary integrated conceptual aircraft design and optimization) [5]. The tool consists of different modules, which are written in C++, to size the main aircraft components, analyze the performance of the aircraft and evaluate the final design at the end. The design process aims to fulfill predefined top-level aircraft requirements (e.g., range, cruise speed, cruise altitude). The different modules read the required input data from a central aircraft data file in the XML-format and subsequently write their results into the same file, such that successive tools can read them. In addition to the semi-empirical equations for the determination of the aircraft component masses, an external tool, based on semi-empirical and analytic methods, is included to determine the effects of the additional powertrain components on the wing mass [6]. The multi-liftingline tool LIFTING_LINE of the German Aerospace Center [7] calculates the lift forces and induced drag taking the induced propeller velocities from a blade element momentum theory into account. Additional drag components, such as the viscous drag, result from semi-empirical methods. Recent developments include a new propulsion system library, that enables the modeling of modular hybrid-electric powertrains [8]. The different powertrain components for the reference aircraft and the partial turboelectric aircraft (propeller, gas turbine, generator, electric motor) are modeled by the commercially available tool GasTurb. [4, 6, 9]. The module for system analysis considers the different aircraft systems to determine their mass and their power consumption. At the end of one design iteration, a mission analysis uses the estimated masses, the aerodynamic polars, the system power demands and the powertrain characteristics to calculate the aircraft's flight condition at each step of the design mission. The modules for component sizing and performance analysis are executed iteratively till a converged design is reached.

2.2. Reference aircraft (REF 2025)

The methods described before are used to redesign a Beechcraft 1900D, which had the most flight hours in Europe in 2019 and was therefore selected as the reference aircraft [10]. The Beechcraft 1900D had its first flight in 1990, is equipped with a pressurized cabin and mechanical flight controls and uses two turboprop engines with four bladed constant speed propellers to generate thrust [6, 11, 12]. The maximum take off mass of the Beechcraft 1900D is below 8618 kg (7765 kg), which allows a certification under CS 23 regulations [13]. During the last 30 years, a lot of progress in increasing the efficiency of gas turbines and electrical systems has been made. To take these improvements for the conventionally driven reference aircraft into account, an updated version of the reference aircraft with an entry into service in 2025 is designed. The assumed changes in the mass of the operating items, the electric system and the specific fuel consumption (SFC) of the powertrain are listed in Tab. 1.

TAB 1. Assumed Technology progress from 1990 to 2025 [6]

Parameter	EIS 1990	EIS 2025	Change
Operating items mass	533 kg	450 kg	-15.6 %
Electric system mass	145 kg	123 kg	-15.2 %
SFC of the powertrain at cruise	13.66 $\frac{g}{kNs}$	10.63 $\frac{g}{kNs}$	-22.2 %

Within a technology selection process the integration of wingtip propellers in the partial turboelectric design was selected. The integration of the propellers at the outboard wing requires a ground clearance, that is not achievable with the low-wing configuration of the reference aircraft. Hence, the partial turboelectric aircraft has a high-wing configuration. This configuration was transferred to the reference aircraft in Fig. 1 to have a fair comparison. In cruise, the aircraft flies at Mach 0.4 in an altitude of 23,000 ft. Further top level aircraft requirements include a design range of 510 NM at a payload of 1767 kg and additional reserves for 45 min holding and an alternate flight of 100 NM. Investigations on potential flight routes and optimum operating strategies resulted in a average study mission, which describes the transportation of 14 passengers (1325.25 kg) over a distance of 257 NM. The flight in a optimized cruise altitude of 25,000 ft takes 1.17 hours.

2.3. Partial turboelectric aircraft (PT 2025)

Based on the conventional reference aircraft in 2025, a partial turboelectric version of the aircraft with wingtip propellers was designed. Within the powertrain, the gas

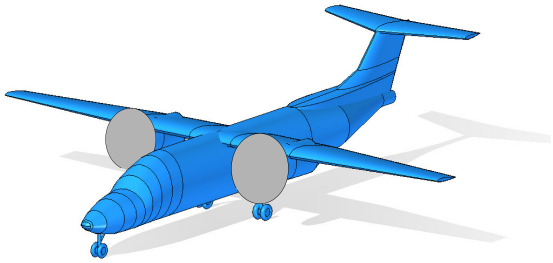

FIG 1. Reference aircraft in 2025

turbine at each wing half drives a propeller and a generator to provide power to an electric motor at each wing tip as shown in Fig. 2. One half of the gas turbine's shaft power drives directly a propeller, whereas the other 50 % of the shaft power is transformed by the generator.

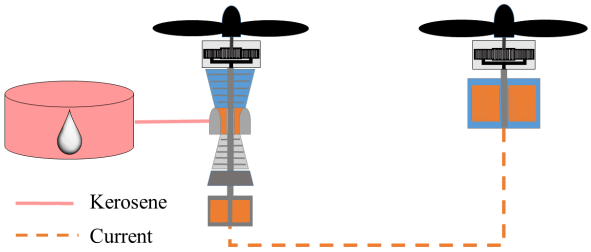

FIG 2. Partial turboelectric powertrain

The four propellers are installed at the wing leading edge (tractor configuration) and rotate against the wing vortex of the respective wing half. Previous CFD simulations for different positions of the conventionally driven propeller and the electrically driven wingtip propeller have shown that the greatest aerodynamic efficiency is reached when the conventionally driven propeller is located close to the wingtip propeller [3]. Consequently, both gas turbines move to the outboard wing. Additional flutter simulations have confirmed a flutter clearance of the wing structure inside the flight envelope. The resulting design is depicted in Fig. 3.

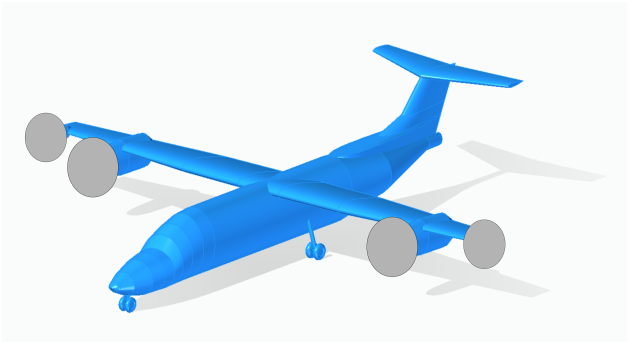

FIG 3. Partial turboelectric aircraft with winp tip propellers

3. EMISSION AND COST ESTIMATION

This chapter describes the methodologies to evaluate the new aircraft designs in terms of CO_2- and NO_X- emissions as well as life cycle costs (in USD). The life cycle costs include the whole aircraft lifespan from development over production and operation to the end of the product lifetime. All costs are related to the year 2020. Since the different cost models are based on data from different years, the U.S. consumer price index is used to convert the results of different cost models to the year 2020 [14].

3.1. CO_2 and NO_X emissions

Previous ecologic life cycle analyses have shown that over 90 % of the emissions occur during the operational phase of an average aircraft life. Hence, this study takes only the CO_2- and NO_X-emissions during operation into account. Simplifying, they can be determined by constant factors for each burned kilogram of kerosene. Tab. 2 shows the factors for CO_2 and NO_X emissions that occur during the production and combustion of one kilogram kerosene.

TAB 2. Equivalent emissions and costs associated with production, provision and use of kerosene in 2020

Scenario parameter	Eq. emissions [kg]
1 kg Kerosene	
CO_2	3.6387
NO_X	0.00184

3.2. Operating costs

The operating costs can be divided into direct and indirect operating costs. In this study, direct operating costs include charges for navigation, ground handling and landing, depreciation, crew salaries, maintenance and fuel costs and insurance premiums. Indirect operating costs cover costs for catering, ticket sales, advertising and general administration. The cost estimate for the conventional aircraft components is taken from the methodology for the Central Reference Aircraft System (CeRAS), which was set up at the Institute [15].

3.2.1. Direct operating costs

Navigation charges for Germany are taken from Eurocontrol [16] and are normalized to the maximum take off mass and distance flown [17]. A regression analysis of 425 different airports provide cost estimating relationships for ground handling and landing depending on maximum take off mass and number of passengers [18]. To estimate the annual depreciation, the study assumes that the aircraft will be taken out of service after 20 years. Currently, the reference aircraft Beechcraft 1900D with an age of over 20 years is still traded for 50 % of the original price. This results in an annual depreciation of 2.5 %. The annual depreciation rate is multiplied by the aircraft list price, which is based on a regression analysis of selected aircraft parameters according to [19]. In an economic evaluation of the aviation market, the FAA lists the average annual salary of commercial pilots with 173,270 USD in 2018 [20]. A commercial pilot flies 75 hours per month according to the U.S. bureau of labor statistics, which leads to a wage of 193 USD per hour [21]. Since the Beechraft 1900D flies without cabin attendants, the crew costs include only pilot salaries. The estimation of the maintenance cost distinguishes between the maintenance of the aircraft and the maintenance of the powertrain. The airframe and gas turbine overhaul costs are based on the estimation from Harris [22], which uses the reports of 67 airlines to the U.S. Department of Transporta-

tion in 1999. The derived cost estimating relationships from Harris include the number of aircraft in the operator's fleet. Because the evaluation of the aircraft design does not take the operator's fleet composition into account, the number of aircraft in the operator's fleet is neglected in the modified equations 1 and 2 [23].

$$MC_{Airframe} = K[(OEM \cdot 2.2046)^{0.72118} \cdot FH^{0.46050} \cdot FC^{0.32062} \cdot (1+\Phi_{Airframe})^{-0.43177}] \quad (1)$$

The factor K in both equations 1 and 2 considers the service type of the aircraft (passenger or cargo), the aircraft age (maturity of technology), the type of engine (turbofan or turboprop) and an additional airline cost factor. For the considered passenger aircraft with turboprop engines, the authors assume an early aircraft model and above-average airline costs, which result in a factor K of 2.02. $\Phi_{Airframe}$ describes the share of the maintenance activities that are undertaken by the operator. All maintenance work at the airframe are assumed to be executed at the aircraft operator, which means that $\Phi_{Airframe}$ is one. Further input parameters are the operating empty mass empty of the aircraft (OEM), the flight hours per year (FH) and number of flights per year (FC). Analog to Eq. 1, Eq. 2 describes the maintenance cost of a gas turbine.

$$MC_{Gasturbine} = K[(SLST \cdot 0.22473)^{0.8965} \cdot N_{Gasturbines}^{0.9234} \cdot FH^{0.15344} \cdot FC^{0.37535} \cdot (1+\Phi_{Gasturbines})^{-0.34704}] \quad (2)$$

Eq. 2 described originally the maintenance costs of engines that were of the type turbofan or turboprop. In a partial turboelectric power train architecture, the gas turbines shall provide not only thrust but also power. In this case, the equivalent sea level static thrust ($SLST$) of the gas turbine's shaft power, that can drive a propeller and a generator, has to be determined. Raymer describes following equation to determine the sea level static thrust based on the available shaft power [24].

$$SLST = \frac{C_T}{C_P} \cdot \frac{P}{nD} \quad (3)$$

The equation uses the shaft power P, the diameter D and the rotational speed n of the propeller as well as the ratio of the propeller's thrust and power coefficient $\frac{C_T}{C_P}$. Raymer refers to an existing correlation between $\frac{C_T}{C_P}$ and C_P of a three bladed propeller in the range from $C_P = 0$ to $C_P = 0.35$ to determine $\frac{C_T}{C_P}$. Since this correlation is illustrated in form of a diagram, an analytic function (Eq. 4) has been derived from this graph for $C_P > 0.5$.

$$\frac{C_T}{C_P} = -108.06C_P^3 + 89.616C_P^2 - 27.881C_P + 3.7778 \quad (4)$$

Besides the maintenance of the gas turbine, the propellers, generators and electric motors cause additional maintenance costs in a partial turboelectric powertrain. Propellers must be regularly shipped to a maintenance shop for inspections and overhaul. A report about the Sensenich Propeller Services in Georgia [25] tells that the overhaul of a full-feathering turboprop, which is typically every 1000 to 2000 flight hours, costs 7000 USD or more. After the second overhaul, the propeller blades have to be replaced. The cost for inspection and replacement can be expressed by following Eq. 5.

$$MC_{Propeller} = 4.67 \cdot FH + \frac{FH}{4500} \cdot p_{Propeller} \quad (5)$$

To estimate the maintenance cost for propeller an average time between overhaul (TBO) of 1500 flight hours (FH) was assumed. The price estimation of a new propeller $p_{Propeller}$ will be described in section 3.3.2.
The technical structure of an electric motor and a generator are quite similar. Thus, the same maintenance cost relationship can be applied for both components. The aircraft manufacturer Pipistrel provides helpful cost estimations for potential customers of their two-seater all-electric aircraft 'Alpha Electro' [26]. In October 2017, the overhaul of the 60 kW electric motor, which is required after 2000 flight hours, cost 587.8 USD plus twelve hours of labor. After 6000 flight hours the electric motor has to be replaced. Due to higher cost for larger engines, the maintenance cost from Pipistrel were scaled linearly by the design power of the electric machine $P_{ElectricMachine}$ in Eq. 6.

$$MC_{ElectricMachine} = [(W_{Mechanic} * 12 + 587.8) \cdot \frac{FH}{2000}] \cdot \frac{P_{electricMachine}}{60} + \frac{FH}{6000} \cdot p_{ElectricMachine} \quad (6)$$

Analog to the price of a new propeller, the price estimation of a new electric machine $p_{electricMachine}$ will be described in section 3.3.2. The wage of a mechanic $W_{Mechanic}$ was assumed to be similar to a manufacturer, whose hourly wage was 98 USD in 2012, according to Raymer. In their economic evaluation of the aviation market, the FAA assumed a price of 4.73 USD per gallon for Jet A fuel in 2018 [20]. This price does not take bulk purchases into account and is therefore typical for smaller operators. The yearly insurance premium is assumed to be 1 % of the purchase price of the aircraft. To validate the described methods, a database from Conklin & de Decker [27], which lists the current operating cost of a Beechcraft 1900D, was used. Their values for fuel, maintenance, crew and insurance cost were converted to the year 2018 and compared to the results of the implemented cost estimating relationships.

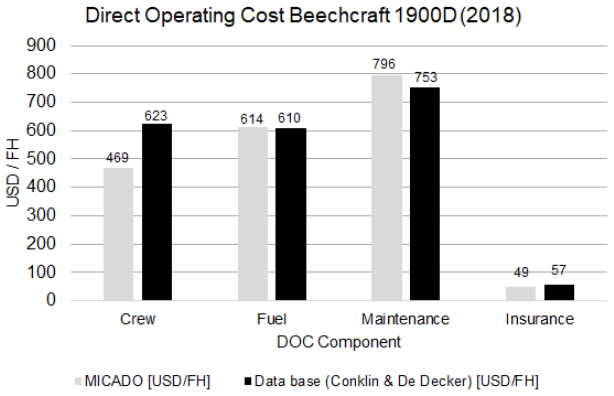

FIG 4. Comparison of direct operating cost of the Beechcraft 1900D in 2018

The crew cost are underestimated by 24.7 %, because additional benefits are not included in the yearly salary of airline

pilots in the FAA's report [20]. According to Conklin & de Decker they contribute to 21.7 % of the yearly crew cost. As the assumed fuel price of the FAA is based on the same database, the good agreement between the real and estimated fuel costs shows that the fuel consumption of the reference aircraft is close to the real fuel consumption. The maintenance cost are overpredicted by +5.7 %. This may be related to the above average airline cost factor in the constant K of Eq.1 and 2. The insurance cost are lower (-14 %) compared to the value of the database.

3.2.2. Indirect operating cost

To estimate the indirect operating cost a methodology from Kroo is used that is based on studies of the B-747, DC-10 and B-737 [28].

$$IOC = -0.04 + 0.00129 \cdot MTOM + 0.00119 \cdot N_{seat} + 0.0127 \cdot N_{seat} \cdot LF \tag{7}$$

Eq. 7 describes the costs for a domestic route with a range of 1000 NM depending on the maximum take off mass $MTOM$ the number of seats N_{seats} and the seat load factor LF and can be converted for smaller ranges by the following equation.

$$C_{Range} = 638.6 \cdot R^{-1.015} + 0.4325 \tag{8}$$

The estimation from Kroo includes the charges for ground handling and landing as well as passenger handling. These cost items are already considered in the direct operating costs and therefore subtracted from Eq. 7.

3.3. Development, production and end of life costs

Besides the operating costs, the development, production and end of life costs contribute to the life cycle costs.

3.3.1. Development costs

The development costs or non-recurring costs arise independently of the number of produced aircraft. To estimate the development costs, the cost estimation relationships from the DAPCA IV model, which were modified by Raymer [24], are used to estimate the development costs. The method estimates the labor hours for airframe engineering and manufacturing of the test aircraft as well as the cost for development support, materials and quality controls.

3.3.2. Production costs

Except for the costs for the powertrain components, the estimation of the production costs (or recurring costs) rely on a method developed by Beltramo et al. [29]. The equations correlate the productions costs of the main aircraft components and their weight and produced quantity. They provide the cost per aircraft assuming an aircraft manufacturer's profit of 10 %. Due to the electrified powertrain, new estimation methods had to be developed for the individual powertrain components. Based on a price list from the propeller manufacturer Hartzell, a cost relationship between the price of a variable pitch propeller and its mass has been derived to estimate the cost of a new propeller [30].

$$p_{Propeller} = 1030.1 \cdot m_{Propeller}^{0.8351} \tag{9}$$

The estimation of the price for a new gas turbine is based on an existing correlation from Langhans [31]. His correlation takes engines in the range of 'CF34-3B1' (Bombardier Challenger Series) and 'GE90-115B' (Boeing 777) into account. The thrust of the gas turbine of the reference aircraft Beechcraft 1900D (PT6A-67D) is below the thrust of the smallest engine in the database and the application of the unmodified equation from Langhans showed that cost are overpredicted especially for smaller engines. Consequently, the results of the existing correlation are reduced by two million USD, which leads to Eq. 10.

$$p_{Gasturbine} = 0.941 + 0.2603 \cdot \frac{m_{Gasturbine} \cdot 2.2046}{1000} + 0.04765 \cdot \frac{m_{Gasturbine} \cdot 2.2046}{1000} \tag{10}$$

The costs for both, the electric motors and generators, are estimated by Eq. 11.

$$p_{ElectricMachine} = 0.20 \cdot P_{ElectricMachine} \tag{11}$$

The cost factor of 0.2 USD per Watt design power is based on the price for a new electric motor of the Pipistrel Alpha Electro [26]. In October 2017, the manufacturer Pipistrel put the cost of an electric motor with a maximum take off power of 60 kW at 10,000 EUR. At that time, the exchange rate of one Euro was 1.1756 American Dollar [32]. After manufacturing and purchasing the aircraft components, they have to be assembled. According to Beltramo, the assembling of the individual parts increases the total recurring costs by 13 % to 15 % [29]. This study assumes an increase of 15 %.

3.3.3. End of life costs

At the time of decommissioning of the aircraft, the aircraft is flown to the end of life site and dissembled. While valuable components are recycled, the residual aircraft parts are landfilled or incinerated. In her PhD thesis, Katharina Schäfer developed a cost model to estimate the cost of the end of life processes [18]. The transportation to the end of life site is calculated by the previously described operating cost model (see 3.2). A logarithmic function describes the cost for disassembly and dismantling.

$$EOLC_{Disassembly} = \frac{218,800 \cdot OEM}{OEM + 31,600} \tag{12}$$

The costs for landfill and incineration as well as the material's scrap value are related to the mass of the material in the corresponding aircraft component. Tab. 3 shows the assumed material distributions of the main aircraft components.
Except for the material distribution of the electric machines, the material distribution in the aircraft components was determined by the project partners in the project GNOSIS. The material distribution for electrical machines is taken from [33]. To simplify the cost estimation, materials listed in Tab. 3 as 'Other' are assumed to be incinerated. They are mainly rubber in the landing gears and isolation materials in the electric machines. The cost and scrap values of the materials are listed in Tab. 4.
The scrap value for copper is taken from the current price at Greengate Metals in Manchester [34]. 70 % of the aluminum, steel and copper are recycled and then resold,

TAB 3. Material distributions of the main aircraft components

Material [%]	Aircraft components						
	Wing	Fuselage	Tailplane	Fin	Landing gear	Gas turbine	E-Machine
Aluminum	90	94	94	94	11	5	17
Steel	5	3	3	3	73	51	60
Titanium	5	3	3	3	10	7	0
Nickel	0	0	0	0	0	36	0
Copper	0	0	0	0	0	0	9
Other	0	0	0	0	6	1	14

TAB 4. Cost and scrap values of the materials according to [18, 34] in 2010-USD per ton

Material	Costs [USD]		Scrap values [USD]
	Landfill	Incineration	
Aluminum	92.17	-	1,600
Steel	92.17	-	350
Titanium	92.17	-	36,920
Nickel	92.17	-	12,307
Copper	92.17	-	4,000
Other	-	145.15	-

whereas only 50 % of the titanium and nickel are resold. The remaining material share is landfilled.

4. PARAMETER STUDIES

Parameter studies shall reveal the influence of the wing geometry, the flight condition at cruise and the propeller geometry on the costs and the CO_2 and NO_X emissions. The first part of this section describes the selected parameters, while the second part will analyze their effect on the emissions and costs.

4.1. Selected parameters

Five aircraft parameters were selected to perform the parametric studies.

Wing aspect ratio
The wing aspect ratio has a great influence on the induced drag of the wing. For the same lift coefficient of the wing, higher aspect ratios decrease the induced drag. The electrification of the powertrain, on the other hand, facilitates the integration of propellers at the wing tip, which can reduce the induced drag analog to an increasing wing aspect ratio. Thus, this study shall show which approach leads to lower emissions and costs. The aspect ratio ranges from -15 % to +20 % relative to the original aspect ratio of 9.16 and changes by 5 % at each step.

Cruise Mach number and altitude
A lower dynamic pressure requires a higher lift coefficient to stay in a stationary flight condition, and vice versa. For a constant wing geometry, higher lift coefficients lead to a quadratic increase of the induced drag and the same considerations apply as for the wing aspect ratio. Moreover, the flight speed influences the propulsive efficiency of the propellers and consequently the fuel consumption. The cruise altitude of the considered study mission, which is constant during one mission, starts at the maximum cruise altitude of 25,000 ft and decreases to 20,000 ft passing the different altitudes in a step width of 500 ft. The original cruise Mach number of 0.4 is increased to 0.41 and 0.42. Higher values are not feasible because the powertrain can not accelerate to higher cruise Mach numbers. On the other hand, the required descend speed of 220 KCAS cannot be reached in the mission analysis of MICADO if the cruise Mach number is below 0.4.

Propeller rotational speed and diameter
The rotational speed and diameter of the propeller influence the propulsive efficiency of the propeller and consequently the fuel consumption of the powertrain. Moreover, the rotational speed and diameter of the wing tip propeller has an impact on the potential induced drag reduction. Greater propeller diameters require lower rotational speeds, whereas smaller diameters require higher rotational speeds. The default propeller diameter of the partial turboelectric aircraft is 2.275 m, with the propeller rotating at 1800 rpm during cruise. The product of these two parameters is kept constant. This results in following diameter and rotational speed pairs in Tab. 5.

TAB 5. Propeller diameters and related rotational speeds

Propeller diameter [m]	**Rotational speed in cruise [rpm]**
2.2	1861
2.25	1820
2.3	1780
2.35	1743
2.4	1706

4.2. Results and discussion

The following results of the parameter studies describe the relative change with respect to the conventionally operated reference aircraft in 2025. The reference aircraft, which has a wing aspect ratio of 9.16, flies at Mach 0.4 in 25,000 ft during cruise. In cruise, the propellers of the reference aircraft, which have a diameter of 2.794 m, rotate at 1400 rpm.
Fig. 5 plots the relative change of the emissions and total operating costs for different wing aspect ratios of the reference and partial turboelectric aircraft in 2025.
Both designs emit less CO_2 and NO_X if the wing aspect ratio increases. Although the integration of additional propellers at the wingtip increases the maximum lift to drag ratio in cruise between 2.7 % and 4.4 %, the poorer power efficiency of the electric powertrain in the partial turboelectric powertrain leads to higher emissions of the PT 2025 than the REF 2025 design. During the complete mission, the efficiency of the electrical powertrain, which is assumed to comprise the gas turbine, generator, cable, switch, electric motor, gearbox and propeller, is lower than the efficiency of the conventional powertrain, see Fig. 6. Because the higher lift to drag ratio and the heavier partial turboelectric aircraft reduce the required thrust of the electrified aircraft only by 2 % during cruise, the poorer efficiency of the partial turboelectric powertrain results in a higher fuel consumption.
The additional maintenance of the partial turboelectric powertrain components increase the total operating costs of the PT 2025 by approximately 1 % compared to the reference aircraft. The lower fuel costs at higher aspect ratios com-

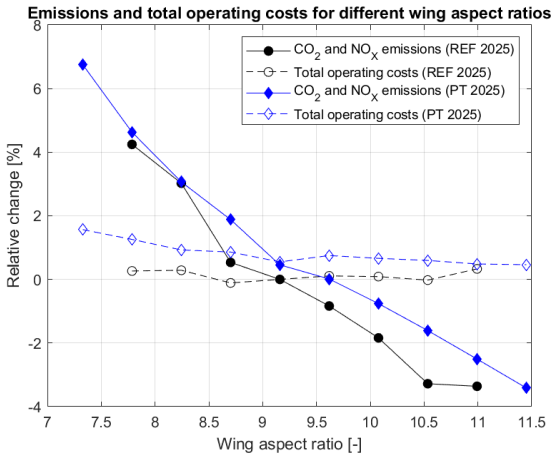

FIG 5. Emissions and total operating costs for different wing aspect ratios

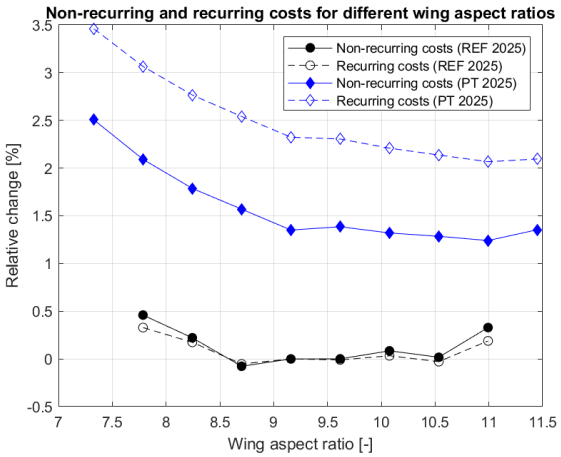

FIG 7. Non-recurring and recurring cost for different wing aspect ratios

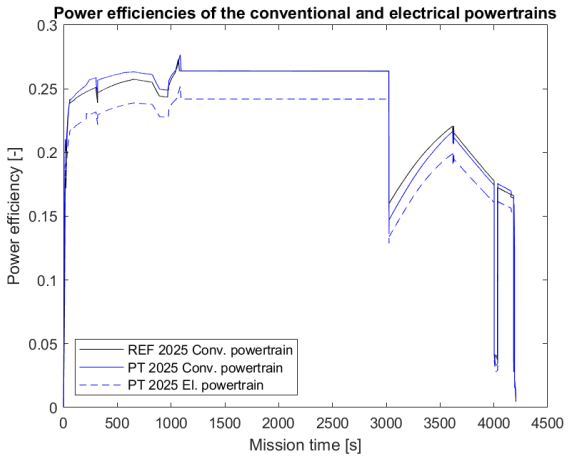

FIG 6. Powertrain efficiencies of the conventional and electrical powertrains

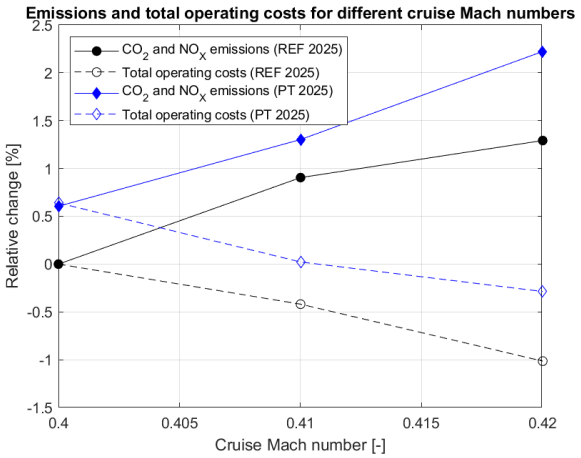

FIG 8. Emissions and total operating costs for different cruise Mach numbers

pensate the higher depreciation costs, which result from the higher aircraft list price. The electric motors and generators increase the recurring costs of the PT 2025 by 2 % to 3.5 % in Fig. 7, as well. The higher operating empty mass of the partial turboelectric aircraft results in higher non-recurring cost (1.24 % to 2.51 %). Since the operating empty mass increases for aspect ratios smaller 9, both cost components increase.

Following the studies on different wing aspect ratios, the cruise speed and altitude during the study mission are varied. Fig. 8 shows that the CO_2 and NO_X emissions rise with higher Mach numbers. The increased thrust at higher cruise speed leads to higher fuel consumption and emissions. On the other hand, the shorter mission time reduces the pilot costs and consequently the operating cost.

The cruise altitude has a strong effect on the required thrust as well. Flying at higher altitudes reduces the drag and the required thrust. Thus, the emissions of CO_2 and NO_X decline in Fig. 9. However, between an altitude of 21000 ft and 22000 ft, the lower efficiency of the gas turbine at higher altitudes leads to a slight increase of the fuel consumption and consequently emissions. As the cruise altitude has no strong influence on the flight time, the operating cost increase only slightly by 0.5 % at higher altitudes.

Finally, the diameters of the four propellers of the partial turboelectric aircraft are varied. During the climb and cruise phase, the propellers with a greater diameter have a higher

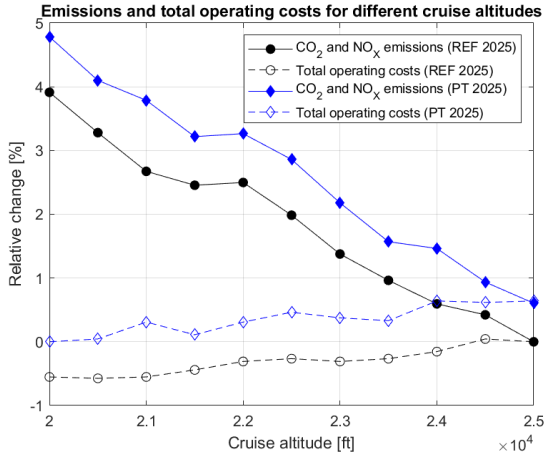

FIG 9. Emissions and total operating costs for different cruise altitudes

propulsive efficiency. This leads to a lower fuel consumption and consequently lower emissions in Fig. 10. However, propellers with greater diameters are more expensive and increase the maintenance cost of the aircraft. Thus, higher operating costs occur.

The same effect can be seen at the recurring costs in Fig. 11. Related to the greater diameter are heavier

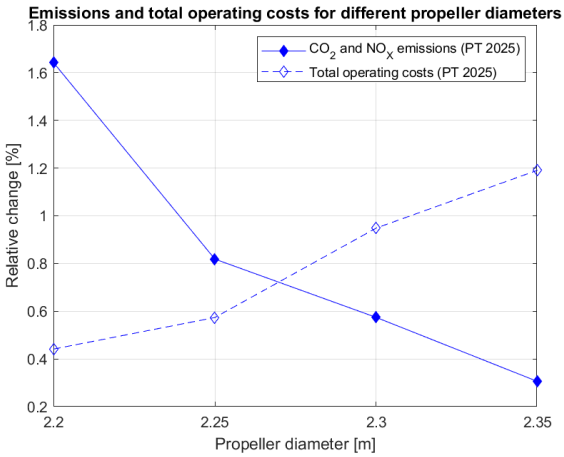

FIG 10. Emissions and total operating costs for different propeller diameters

propellers. The heavier propellers increase the overall operating empty mass of the aircraft, which changes from 4682 kg for the aircraft with a propeller diameter of 2.2 m to 4703 kg for the aircraft with a propeller diameter of 2.35 m. This increases the non-recurring and recurring costs of the partial turboelectric aircraft.

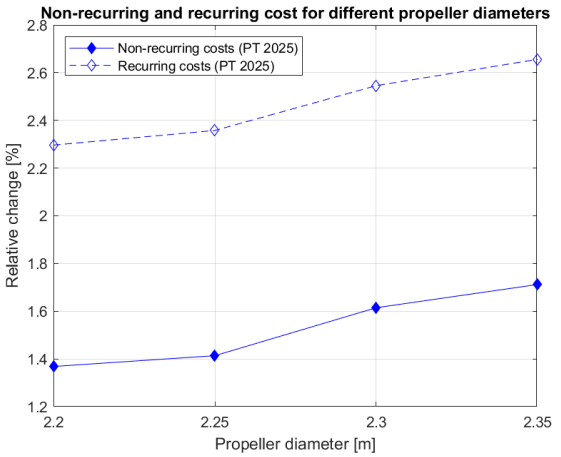

FIG 11. Non-recurring and recurring costs for different propeller diameters

5. CONCLUSION

To analyze the effect of different wing aspect ratios, cruise speeds and altitudes as well as propeller diameters on the emissions and costs of a partial turboelectric aircraft, existing cost relationships have been adapted and extended for new electrified aircraft concepts. The separate variation of each parameter has shown that the conventionally driven aircraft emits less emissions and is cheaper than the partial turboelectric aircraft, both with an entry into service in 2025. Even though the electrically driven wingtip propellers can increase the maximum lift to drag ratio during cruise by 2.7 % to 4.4 %, the poor power efficiency of the electrical powertrain leads to a higher fuel consumption and hence emissions. The additional powertrain components at the partial turboelectric aircraft results in higher maintenance, production and non-recurring costs. In general, the changes in wing aspect ratio, altitude, and flight speed result in similar trends of emissions and costs for the reference aircraft and the partially turboelectric aircraft. Future work shall include the variation of the hybridization degree of the partial turboelectric powertrain to explore if smaller electrical powertrains can achieve a disproportionate reduction of the induced drag. This requires the adaption of the propeller geometry to the new thrust distribution.

6. ACKNOWLEDGEMENTS

The results were developed within the project GNOSIS, which is funded by the sixth call in the aeronautical research program (’Luftfahrtforschungsprogramm’) of the German Federal Ministry for Economic Affairs and Climate Action.

References

[1] H. Ritchie. Climate change and flying: what share of global CO2 emissions come from aviation?, 2020. https://ourworldindata.org/co2-emissions-from-aviation.

[2] D. S. Lee, D. W. Fahey, A. Skowron, M. R. Allen, U. Burkhardt, Q. Chen, S. J. Doherty, S. Freeman, P. M. Forster, J. Fuglestvedt, A. Gettelman, R. R. de León, L. L. Lim, M. T. Lund, R. J. Millar, B. Owen, J. E. Penner, G. Pitari, M. J. Prather, R. Sausen, and L. J. Wilcox. The contribution of global aviation to anthropogenic climate forcing for 2000 to 2018. *Atmospheric environment*, 244(1), 2020. DOI: 10.1016/j.atmosenv.2020.117834.

[3] C. Zumegen, P. Strathoff, E. Stumpf, J. van Wensveen, C. Rischmüller, M. Hornung, I. Geiß, and A. Strohmayer. Technology selection for holistic analysis of hybrid-electric commuter aircraft. *CEAS Aeronautical Journal*, 13(3):597–610, 2022. DOI: 10.1007/s13272-022-00589-z.

[4] P. Strathoff, C. Zumegen, E. Stumpf, C. Klumpp, P. Jeschke, K. L. Warner, R. Gelleschus, T. Bocklisch, B. Porter, L. Moser, and M. Hornung. On the Design and Sustainability of Commuter Aircraft with Electrified Propulsion Systems. In American Institute of Aeronautics and Astronautics, editor, *AIAA AVIATION 2022 Forum*, 2022. DOI: 10.2514/6.2022-3738.

[5] K. Risse, E. Anton, T. Lammering, K. Franz, and R. Hoernschemeyer. An Integrated Environment for Preliminary Aircraft Design and Optimization. In American Institute of Aeronautics and Astronautics, editor, *53rd AIAA/ASME/ASCE/AHS/ASC Structures, Structural Dynamics and Materials Conference: SciTech 2012*, volume AIAA 2012-1675. AIAA, 2012. DOI: 10.2514/6.2012-1675.

[6] C. Zumegen, P. Strathoff, E. Stumpf, M. Schollenberger, T. Lutz, E. Krämer, B. Kirsch, J. Friedrichs, M. Schubert, A. Dafnis, and K.-U. Schröder. Aerodynamic and structural analysis of a partial turboelectric commuter aircraft with wingtip propellers at aircraft level. In American Institute of Aeronautics and Astronautics, editor, *AIAA AVIATION 2022 Forum*, 2022. DOI: 10.2514/6.2022-3955.

[7] K. H. Horstmann, T. Engelbrecht, and C. M. Liersch. LIFTING_LINE: Version 3.0: Handbook, 2019.

[8] B. Aigner, M. Nollmann, and E. Stumpf. Design of a Hybrid Electric Propulsion System within a Preliminary Aircraft Design Environment. In Deutsche Gesellschaft

für Luft- und Raumfahrt - Lilienthal - Oberth e.V., editor, *67. Deutscher Luft- und Raumfahrtkongress*, 2018. DOI: 10.25967/480153.

[9] GasTurb GmbH. User Manuals: GasTurb 14 Manual, 2022.

[10] OAG Aviation Worldwide Limited. Airline Schedules Data, 2020. https://www.oag.com/airline-schedules-data.

[11] Raytheon Aircraft Company. Pilot Operating Handbook Beechcraft 1900D, 2006.

[12] M. Lambert. *Jane's All the World's Aircraft 1990-91*. Jane's Information Group, 1990. ISBN: 978-0710609083.

[13] European Aviation Safety Agency. Certification Specifications for Normal-Category Aeroplanes CS-23: Amendment 5, 2017.

[14] U.S. Bureau of Labor Statistics. CPI for All Urban Consumers (CPI-U): Report, 2022.

[15] Kristof Risse, Katharina Schäfer, Florian Schültke, and Eike Stumpf. Central Reference Aircraft data System (CeRAS) for research community. *CEAS Aeronautical Journal*, 7(1):121–133, 2016. ISSN: 1869-5582. DOI: 10.1007/s13272-015-0177-9.

[16] EUROCONTROL. Adjusted unit rates applicable to January 2020 flights, 2020.

[17] EUROCONTROL. Central Route Charges Office: Customer Guide to Charges, 2020.

[18] K. Schäfer. *Conceptual Aircraft Design for Sustainability*. Dissertation, RWTH Aachen University, Aachen, Germany, 2018.

[19] T. Lammering, K. Franz, K Risse, R. Hoernschemeyer, and E. Stumpf. Aircraft Cost Model for Preliminary Design Synthesis. In American Institute of Aeronautics and Astronautics, editor, *50th AIAA Aerospace Sciences Meeting including the New Horizons Forum and Aerospace Exposition*, 2012. DOI: 10.2514/6.2012-686.

[20] Federal Aviation Administration. ECONOMIC VALUES FOR FAA INVESTMENT AND REGULATORY DECISIONS: A GUIDE: 2021 Update, 2021.

[21] U.S. Bureau of Labor Statistics. Airline and Commercial Pilots: Work Environment, 2022. https://www.bls.gov/ooh/transportation-and-material-moving/airline-and-commercial-pilots.htm#tab-3.

[22] F. Harris. An Economic Model of U.S. Airline Operating Expenses, 2005.

[23] T. Schürmann. *Entwicklung eines Betriebskostenmodells für Verkehrsflugzeuge*. Student thesis, RWTH Aachen University, 2008.

[24] D. P. Raymer. *Aircraft Design: A conceptual approach*. AIAA education series. American Institute of Aeronautics and Astronautics, Inc., Reston, Va., 2018. ISBN: 9781624104909.

[25] L. Anglisano. Propeller Overhauls: Neglect Shortens TBO, 2020. https://www.aviationconsumer.com/maintenance/propeller-overhauls-neglect-shortens-tbo/.

[26] Pipistrel. AIRCRAFT INFORMATION Pipistrel ALPHA ELECTRO, 2017.

[27] Conklin & de Decker Associates. Aircraft Operating Cost and Performance Guide: Beechcraft King Air Beech 1900D, 2022. https://conklindedecker.jetsupport.com/details/Beechcraft%20King%20Air%20Beech%201900D.

[28] I. M. Kroo and J. J. Alonso. Aircraft Design: Synthesis and Analysis: Lecture, 2001. http://rahauav.com/Library/Design-performance/Aircraft%20Design,%20synthesis%20and%20analysis.pdf.

[29] M. N. Beltramo, D. L. Trapp, B. W. Kimoto, and D. P. Marsh. Parametric study of transport aircraft systems cost and weight: Report, 1977.

[30] Hartzell Propeller Inc. 2020 Price List, 2020. https://hartzellprop.com/wp-content/uploads/2020-Price-List.pdf?msclkid=2bb7518db4cd11ec8cafcb8a17a9b2df.

[31] S. Langhans. *A Systems Engineering Approach for Economic Assessment of Air Transportation Concepts*. PhD thesis, Hamburg University of Technology, 2013.

[32] European Central Bank. Euro foreign exchange reference rates: US dollar (USD), 2022. https://www.ecb.europa.eu/stats/policy_and_exchange_rates/euro_reference_exchange_rates/html/eurofxref-graph-usd.de.html.

[33] A. Rassõlkin, A. Belahcen, A. Kallaste, T. Vaimann, D. Vyacheslavovich Lukichev, S. Orlova, H. Heidari, B. Asad, and J. Pando Acedo. Life cycle analysis of electrical motor-drive system based on electrical machine type. *Proceedings of the Estonian Academy of Sciences*, 69(2):162–177, 2020. DOI: 10.3176/proc.2020.2.07.

[34] Greengate Metals. Braziery Copper Scrap Metal Manchester, 2022. https://www.greengatemetals.co.uk/scrapmetal/Braziery+Copper.html.